The molecular basis of metabolic syndrome: studies in zebrafish

Nowik, N.

Chapter 2

A comparative transcriptome study of the effects of knock down of the Ptpn6 protein by treatment with morpholino or inhibitor NSC-87877 during mycobacterial infection in zebrafish larvae

Natalia Nowik, Marcel J.M. Schaaf, Herman P. Spaink

Abstract

Protein tyrosine phosphatases play an important role in many cellular processes such as cell survival, migration and immune responses. Protein tyrosine phosphatase nonreceptor type 6 (Shp-1/Ptpn6) knockdown in zebrafish larvae has previously been shown to result in immune deficiency and autoimmune disorders. In the present study, we compared the effects of *ptpn6* morpholino knockdown and the Ptpn6 inhibitor NSC-87877 on zebrafish embryos infected with *Mycobacterium marinum* and performed RNA sequencing (RNAseq) analysis on whole larvae. Infection data showed that mycobacterial infection progressed more rapidly after morpholino and NSC-87877 treatment compared to the control treatment, with the morpholino showing a larger effect than the inhibitor. The RNAseq analysis showed similar patterns in functional annotations and signaling pathways, such as synaptic transmission, ion transport, cell structure, proteolysis, immune response, apoptosis and gonadotropin secretion. Notably, inhibition caused by NSC-87877 and *ptpn6* morpholino knockdown resulted in upregulation of immune related genes. However, there are also some differences, such as, for instance, that *ptpn6* morpholino knockdown had more impact on the expression of metabolic genes. On the other hand, we found a number of genes of which the expression after bacterial infection was not affected by either treatment. The set of genes that show the same transcriptional response after *ptpn6* morpholino knockdown and NSC-87877 inhibitions are a useful reference set that can specifically linked to the function of Ptpn6. The obtained data stimulates further research on the NSC-87877 inhibitor in comparison with other inhibitors of Ptpn6.

Introduction

Protein dephosphorylation is a process that plays a role in all physiological processes inside the cells of living organisms. Dysregulation of this process leads to various diseases, such as cancer, diabetes, autoimmune disorders and neurological diseases[1,2,3,4,5]. The enzymes responsible for this process, protein tyrosine phosphatases (PTPs), form a large family of 107 enzymes divided into 4 groups depending on their protein structure and function[6,7,8,9]. Class I of PTPs is the biggest group and contains non-receptor PTPs. Two highly related proteins of this family are well conserved in vertebrates: Protein Tyrosine Phosphatase, Non-Receptor Type (PTPN)6, and PTPN11. They are also called Src homology region 2 domain-containing phosphatase (SHP)-1 and SHP-2, respectively, because they have two Src homology 2 domains N-terminal to the phosphatase catalytic domain[10] and are regulated by self-phosphorylation. PTPN6 is expressed mainly in the hematopoietic system, but expression has been observed in other cells as well, albeit at lower levels[11]. PTPN6 is also expressed by epithelial cells, and these cells express a different isoform type, which only differ in the first few amino acids that can result in differences in its function[12,]. PTPN6 plays a role in many different signaling pathways in cells. It is a key regulator of myeloid cell function and it impacts the function of diverse cytokine receptors, growth factor receptors and immunoreceptors[10]. PTPN11 is expressed more ubiquitously and is believed to be an essential component in several

oncogene signaling pathways[13]. The expression of PTPN11 is significantly lower in hematopoietic cells than that of PTPN6[14]

The function of the mouse *Ptpn6* gene has been intensively studied in various strains called *motheaten*, which carry a mutation in this gene. Besides a line with a genetically engineered mutation[15], there are also several *motheaten* mouse lines carrying spontaneous mutations. The first discovered spontaneous mutant, known as *me,* was a null mutation, where a frame shift mutation leads to a phosphatase-dead PTPN6[16]. The phenotype of this mutant is characterized by skin lesions and lethality within 6 weeks[17]. The *me* mutant also shows other severe disorders, such as autoimmunity and spontaneous inflammatory responses which are caused by a dysregulation of immune cell function [18]. A second spontaneous mutant strain, called *motheaten viable* (*mev*), survives for approximately 12 weeks and shows a similar phenotype as the *me* mutant, but less severe. In addition, two other *Ptpn6* mouse mutants, *spin* and *meB2*, display similar symptoms, which confirms an important role for PTPN6 in the function of myeloid cells and immune regulation[19].

The zebrafish larval model has several advantages for the modeling of disorders that requires studying the function of the innate immune system separate from the adaptive immune system, since the onset of the latter's activity happens later in zebrafish development[20]. In a previous study, we used a morpholino oligonucleotide knockdown approach in zebrafish larvae to study the function of the *ptpn6* gene. We showed that p*tpn6* deficiency in larval zebrafish results in a decreased ability to control a bacterial infection[21]. Our data showed that *ptpn6* acts as a negative regulator of the innate immune system, and thereby playing a crucial role during the response to a bacterial infection[21]. Moreover, knockdown of *ptpn6* in zebrafish leads to severe edema and skin lesions, resembling the murine *Ptpn6* knockout model.

Mycobacterium marinum, a close genomic relative of *M. tuberculosis*, is a natural pathogen of zebrafish which leads to systemic, chronic infection similar to human tuberculosis[22]. Injection of the pathogen in zebrafish larvae causes aggregation of infected macrophages into granuloma-like structures and the activation of granuloma-specific genes. Furthermore, advantages of zebrafish larvae such as their transparency, gives an opportunity to study natural host–pathogen interactions *in vivo* and to understand early host responses to tuberculous infection[23], in the absence of the adaptive immune system, which is not yet developed in the larvae[24].

In a different study, we demonstrated that morpholino knockdown of *ptpn6* prevents the downregulation of insulin- and immune-relevant genes in hyper-insulinemic zebrafish larvae, showing that Ptpn6 functions at the crossroads of immunity and insulin resistance[25]. In addition, Ptpn6 was shown to play a key role in insulin signaling pathways, acting as a mediator that regulates a switch between the insulin-sensitive and insulin-resistant states after hyperglycemia resistance[25].

In the present study, we have explored the effect of Ptpn6 deficiency in the absence and presence of a *Mycobacterium marinum* infection in zebrafish larvae using transcriptome analysis. Two approaches were used. First, we used the morpholino knockdown approach that we had previously used[21]. Second, looking for possible therapeutic opportunities, we tested a chemical inhibitor (NSC-87877) that has been shown to inhibit PTPN6, PTPN11, Dual specificity phosphatases and immune regulators such as cytokine signaling (SOCS) in human cells[26,27,28,29,30]. By comparing the effects of morpholino and inhibitor treatment we aim to establish a solid view of the role of Ptpn6 in the response to a mycobacterial infection.

Materials and methods

Fish maintenance

Wild type zebrafish of the AB/TL line were handled and maintained according to standard protocols (http://ZFIN.org) and in compliance with the directives of the local animal welfare body of Leiden University. Fertilization was performed by natural spawning at the beginning of the light period. Eggs were collected and grown at 28.5 °C in egg water (60 µg/ml Instant ocean sea salt, Sera Marin).

Morpholino injections

For this study, a *ptpn6* morpholino oligonucleotide (GeneTools, LLC, Philomath, Oregon, USA) was used, which was previously described by Kanwal *et al.*[21] This splice-blocking morpholino induces the deletion of the phosphatase catalytic domain in the Ptpn6 protein. The morpholino (5'-ACTCATTCCTTACCCGATGCGGAGC-3') was diluted to a concentration of 0.08 mM in 1× Danieau's buffer (58 mM NaCl, 0.7 mM KCl, 0.4 mM $MgSO_4$, 0.6 mM $Ca(NO_3)_2$, and 5.0 mM HEPES (pH 7.6)) and 1 nl of the *ptpn6* morpholino solution or a standard control morpholino (5'- CCTCTTACCTCAGTTACAATTTATA-3') was injected into the yolk sac of approximately 60 embryos per experimental group at the 1-2 cell stage using an automated injection system[31] (Life Science Methods, Leiden, Netherlands).

Bacterial injections

The *M. marinum* E11 strain, containing an mCherry expression vector, was grown as described in Carvalho *et al.*[32]. Bacteria were injected as described in Benard *et al.*[33] Injections of *M. marinum* (20–40 CFUs, diluted in PBS containing 2% polyvinylpyrrolidone40 (PVP40)) were performed by injection (1 nl) into the yolk sac of approximately 50 zebrafish embryos per experimental group using an automated injection system (Life Science Methods), and took place around 4 hours post fertilization (hpf). Control embryos were injected with PBS. During injections fish were kept under anesthesia in egg water containing 0.02% buffered 3-aminobenzoic acid ethyl ester (tricaine, Sigma–Aldrich).

NSC-87877 treatment

The larvae were incubated from 4 hpf until 5 dpf in egg water that contained a solution of 10 µM NSC-87877 in egg water and DMSO, as the control group, larvae were incubated, during the same period of time, only in water with DMSO.

Microscopy

A Leica MZ16FA fluorescence stereomicroscope (Leica microsystems, Wetzlar, Germany) equipped with a Leica DFC420C digital color camera was used for imaging of the zebrafish embryos. Embryos were kept under tricaine anesthesia during imaging. The images were analyzed using custom-designed pixel quantification software (previously described by Stoop *et al*.[34]), the results are written to a spread sheet so that further statistical analysis using GraphPad Prism 8 software (GraphPad Software, La Jolla, CA, USA) could be applied to the data.

COPAS analysis

Fluorescence intensities in zebrafish embryos were measured every 24 hours until 5 days post infection (dpi) using the COPAS XL (Union Biometrica, Holliston, Massachusetts, USA). The settings were as follows: photo multiplier tube (PMT) voltage was 650 V for green/red and 0 V for yellow, optical density threshold signal was 975 mV (COPAS value: 50), and the time of flight (TOF) minimum was 320 µs (COPAS value: 800).

RNA deep sequencing (RNAseq)

Thirty larvae at 5 dpi per sample, from three independent experiments, were homogenized in 1 ml of TRIzol reagent (Life Technologies), and total RNA was extracted according to the manufacturer's instructions. A total of 2 µg of RNA was used to make RNAseq libraries using the Illumina TruSeq RNA Sample Preparation Kit v2 (Illumina, Inc., San Diego, CA, USA). The manufacturer's instructions were followed with the exception of two modifications. First, in the adapter ligation step, 1 µl, instead of 2.5 µl, adaptor was used. Second, in the library size-selection step, the library fragments were isolated with a double Ampure XP purification with a 0.7× beads to library ratio (Beckman Coulter, Woerden, The Netherlands). The resulting mRNAseq library was sequenced using an Illumina HiSeq2500 Instrument (Illumina, Inc., San Diego, USA) according to the manufacturer's instructions with a read length of 2×50 nucleotides. Image analysis and base calling were done by the Illumina HCS version 2.0.12. Data analysis was performed using Genetiles software as previously described by Veneman et al.[35] and the Pathvisio software package (http://www.pathvisio.org)[36]. False discovery rate (FDR)-adjusted P values were calculated based on the algorithm of Benjamini & Hochberg (1990)[37]. Significance cutoffs at 1.5-fold change and a P value < 0.05 were used. Gene ontology was analyzed using the program DAVID[38].

Statistics

Statistical significance was analyzed using GraphPad Prism 8 software (GraphPad Software, La Jolla, CA, USA). Differences in total fluorescence intensities were statistically tested by unpaired t-test (comparison between 2 groups) or one-way ANOVA followed by Tukey's comparison test (multiple group comparisons).

Results

Transcriptomic profiling and pathways analysis in non-infected larvae

Knockdown studies of the *ptpn6* gene in zebrafish embryos were performed using a previously described splice-blocking morpholino[21]. The *ptpn6* (or standard control) morpholino was injected into the yolk sac of wild type embryos at the in 1-2 cell stadium (Fig.1). The morphants showed some developmental abnormalities such as smaller eyes and cardiac edema that have already been reported previously by Kanwal *et al.*[21]. The Ptpn6 inhibitor NSC-878777 or vehicle (DMSO) was added at 4 hpf. To characterize similarities between the effects of *ptpn6* morpholino and NSC-87877 treatment we performed an RNAseq based transcriptome analysis of zebrafish larvae at 5 dpf (Fig.1). We found 339 genes that were regulated by both the *ptpn6* morpholino and NSC-87877 treatment (Fig.2A). There were 182 upregulated genes shared between the two treatment groups, whereas 1123 genes were only upregulated in the morpholino group and 637 genes that were only upregulated after NSC-87877 treatment (Fig.2A). We found 157 genes that were downregulated by both treatments, 1704 genes that were only downregulated genes upon morpholino treatment and 325 genes that were only downregulated in the NSC-87877-treated group (Fig.2A). Moreover, from the volcano plots it is visible that more genes were downregulated after *ptpn6* knockdown, whereas upregulation is stronger in the NSC-87877-treated group, and that the morphants show a larger variation in the fold changes and p-values than the larvae treated with NSC-87877 (Fig.2B). In summary, these results show that the morpholino treatment induces a larger transcriptional effect than NSC-87877, regulating approximately 2.5 times more genes, and that approximately 10% of all genes regulated by the morpholino is also regulated by NSC-87877. Functional annotation clustering of the shared 339 genes significantly changed in both groups indicated that both methods of Ptpn6 inhibition affected regulation of genes associated with skin formation and regeneration (Table 1). Genes involved in processes involving intermediate filaments, keratin type I activity and fin regeneration were significantly enriched in the cluster of downregulated genes regulated by both morpholino- and NSC-87877-treatment (Table 1). Genes involved in neuroendocrine signaling and immunity were significantly enriched among the cluster of upregulated genes. Further analysis showed that the most enriched pathway among the upregulated genes was glyoxylate and dicarboxylate metabolism signaling, that is mainly responsible for biosynthesis of carbohydrates from fatty acids and is a part of the tricarboxylic acid cycle (TCA) cycle[32] (Table 1).

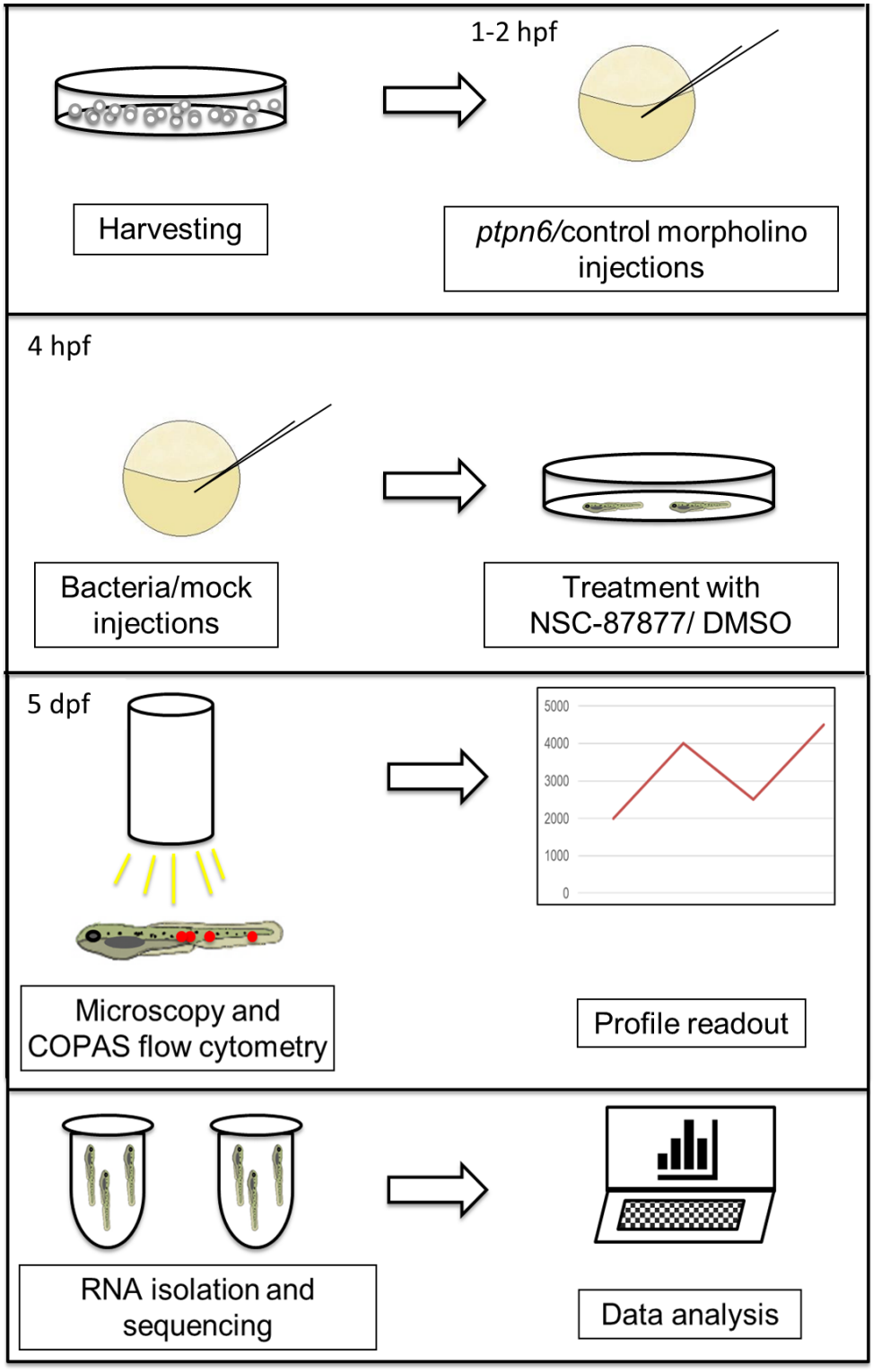

Figure 1. Experimental workflow. Zebrafish embryos were collected and immediately injected with morpholino. After bacterial injection at 4hpi, the embryos were kept in NSC-87877 or DMSO as a control. The bacterial burden was monitored using fluorescence microscopy and COPAS flow cytometry. At 5 dpi RNA of the larvae was extracted and analyzed by deep sequencing.

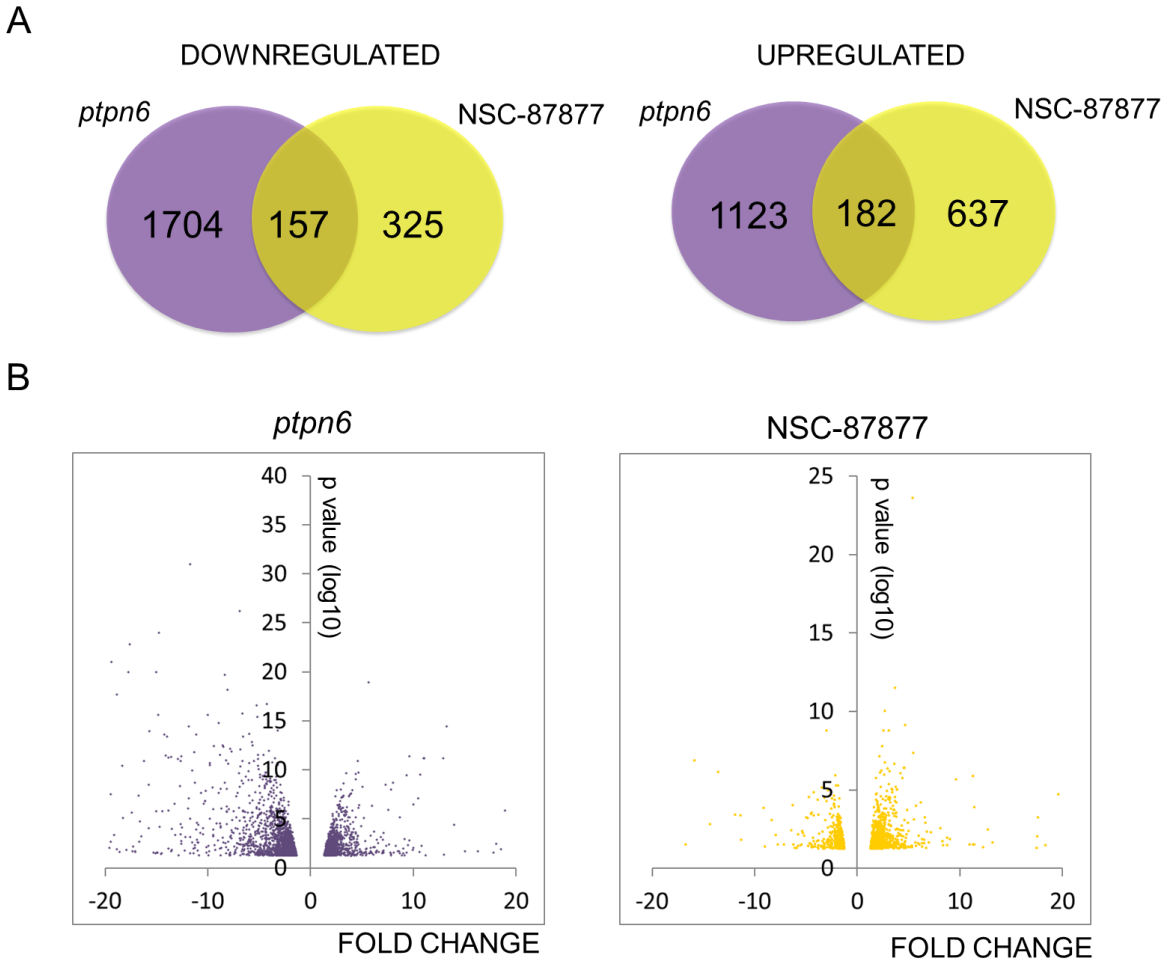

Figure 2. Transcriptome analysis by RNAseq showing modulation of gene regulation induced by *ptpn6* morpholino knockdown and NSC-87877 treatment. RNAseq analysis was performed on 5 dpf larvae treated with either *ptpn6* morpholino or NSC-87877 to inhibit Ptpn6 function. **(A)** Venn diagrams showing (overlaps between) clusters of all genes significantly upregulated or downregulated by *ptpn6* morpholino knockdown (compared to standard control morpholino, violet) or NSC-87877 treatment (compared to vehicle (DMSO) treatment, yellow). **(B)** Volcano plots indicating the fold change (x-axis) and P-value (y-axis) of the regulation for individual genes upon treatment with *ptpn6* morpholino (left panel) or NSC-87877 (right panel).

Morpholino knockdown of *ptpn6* leads to increased bacterial burden and mortality in zebrafish larvae

Zebrafish embryos were infected with *M. marinum* by injection into in the yolk sac at 4 hpf (Fig.1). We have previously shown that granuloma- like aggregates form within the body of the larvae several days post injection using this approach[28]. The infected embryos had been previously injected with the *ptpn6* morpholino or the standard control morpholino. During the infection we monitored the survival of the infected larvae. We found increased infection-induced mortality in the p*tpn6* morphants (~67% at 5 dpi) compared to the group treated with the control morpholino (~20%, Fig.3B).The bacterial burden was monitored for 5 days using COPAS flow cytometry. At 1 dpi there were no significant differences between the groups, with the fluorescence at approximately ~300 AU for all groups. The bacterial burden started

Table 1. Gene ontology analysis of the cluster of genes that are significantly regulated by both morpholino and NSC-87877 treatment using DAVID Functional Annotation Tool (Functional Annotation Clustering and KEGG pathways).

FUNCTIONAL ANNOTATION CLUSTERING		
Enrichment Score	UPREGULATED	DOWNREGULATED
3.15		Intermediate filament Keratin type I Fin regeneration Structural molecule activity
2.23	Neuropeptide hormone Extracellular space	
1.77	Arrestin - like Immunoglobulin E - set	
1.36		Extracellular region Transmembrane region
1.29		Secreted
1.27		Fibronectin, type III
PATHWAYS		
Enrichment Score	UPREGULATED	DOWNREGULATED
4.06	Protein processing in endoplasmic reticulum	
2.15		Tight junction Cell adhesion molecules (CAMs)
0.42		Fructose and mannose metabolism

to raise at 2 dpi up to ~700 AU in control morpholino-treated group, compared to ~1300 AU in the *ptpn6* morphants. At 3 dpi, the difference between the *ptpn6* knockdown group (~2500 AU) and the control group (~1600 AU) started to increase. This tendency continued at 4 dpi with an average ~2700 AU of total fluorescence in the control larvae, compared to ~4300 AU in the Ptpn6-deficient larvae, although large variation between single larvae in the *ptpn6* morpholino-treated group was observed. Finally, the infection results in a significant difference between the control group and the morphant group at 5 dpi (~ 7200 AU versus ~ 13560 AU) (Fig.3A). Similar results were obtained when the bacterial burden was monitored using fluorescence microscopy (Fig.4A). The microscopy data were quantified using pixel count software, showing a significant difference at 5 dpi between the control group (~80 AU) and the *ptpn6 morphants* (~490 AU)(Fig.4B).

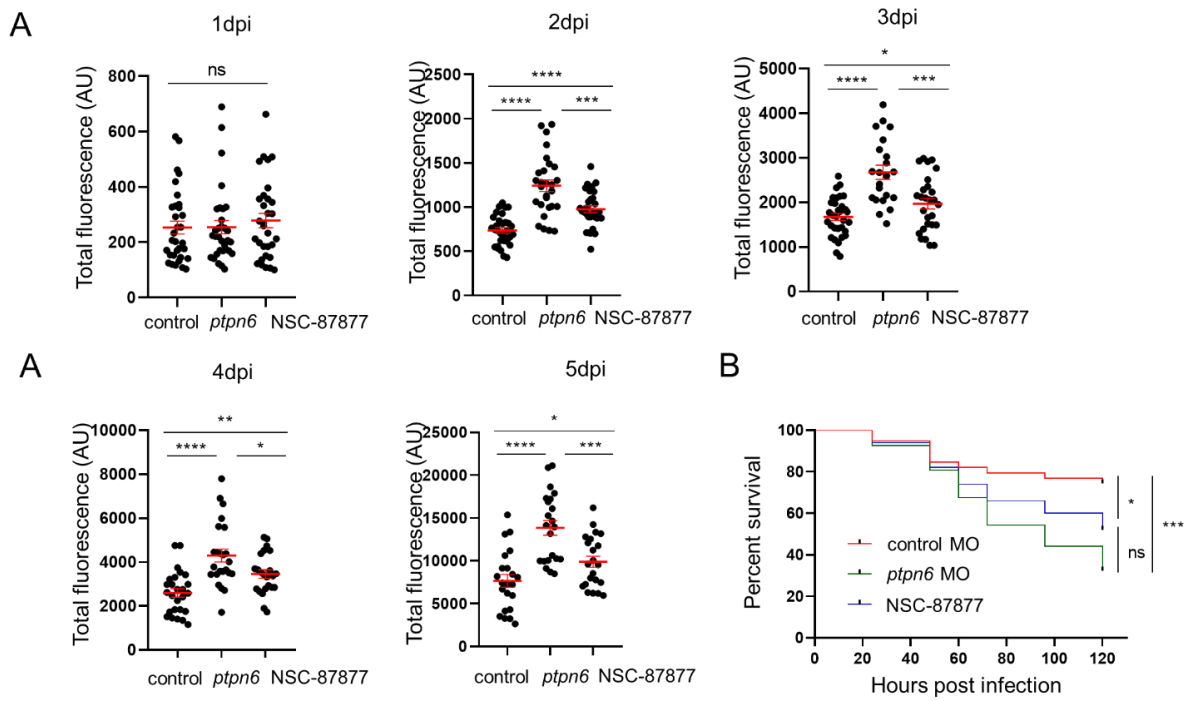

Figure 3. Inhibition of Ptpn6 function increases the bacterial burden and mortality rate after *M. marinum* infection. (A) Bacterial burden in the control, *ptpn6* morpholino- and NSC-87877-treated groups followed up to 5 dpi using COPAS flow cytometry. **(B)** Mortality rate in the control larvae, *ptpn6* morphants and after NSC-87877 treatment after *M. marinum* infection, followed until 5 dpi. Data shown are means ± s.e.m. from three independent experiments. Statistical significance is indicated as *P<0.05; **P<0.01; ***P<0.0 01; ****P<0.0001 (determined using ANOVA with Tukey's post hoc test).

Inhibition of Ptpn6 by NSC-87877 leads to a similar, but smaller, increase in infection rate as *ptpn6* morpholino knockdown

Next, we studied the effect of the Ptpn6 inhibitor NSC-87877 in four different concentrations of the drug (5, 10, 20 and 50 µM). The highest concentration resulted in rapid progression of the infection and enhanced mortality that reached 100% after 2 dpi, whereas 5 µM concentration showed no significant effect during infection (Suppl.fig.1). Treatment with 20 µM of the compound resulted in similar bacterial burdens and mortality rates and the concentration of 10 µM was chosen for further research to study if NSC-87877 has the same effect on the progression of the mycobacterial infection as *ptpn6* morpholino knockdown. Therefore, in the same experiment one group of *M. marinum* infected embryos was treated with 10 µM of NSC-87877 and one group with DMSO as a control (previously injected with control morpholino). Just like *ptpn6* morpholino treatment, NSC-87877 treatment resulted in increased mortality compared to the control-infected group, that reached (~40% at 5 dpi, compared to 65% for the control-treated group, Fig.3B). The progression of the infection was monitored during the following days using COPAS flow cytometry. We did not notice any significant effect of NSC-87877 treatment at 1dpi, but a significant difference was observed

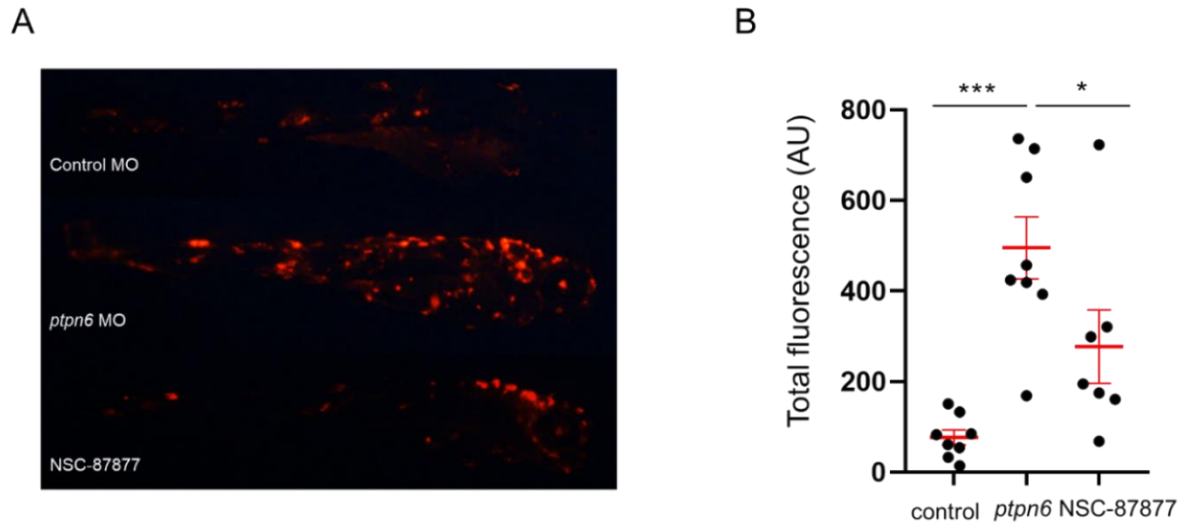

Figure 4. Bacterial burden after *M. marinum* infection. (A) Representative fluorescence microscopy images of bacterial infection in control, *ptpn6* MO- and NSC-87877-treated larvae at 5 dpi. Bacteria are shown in red. **(B)** Pixel counting of bacterial burden in the control/infection, *ptpn6* MO/infection and NSC-87877/infection groups at 5 dpi. Data shown are means± s.e.m. from three independent experiments. Statistical significance is indicated by: *P<0.05; ***P<0.001; (determined using ANOVA with Tukey's post hoc test).

at 2 dpi when a total fluorescence of ~1000 AU was observed in the NSC-87877-treated group (versus ~700 AU in the control group and ~1300 AU in the *ptpn6* morphants). At 3 dpi the difference between the NSC-87877 exposed group (~2000 AU), the control group (~1600 AU) and the *ptpn6* knockdown group (~2500 AU) was increased and this tendency continued at 4dpi with the average total fluorescence of and ~3400 AU in the inhibitor treated larvae (~2700 in the control group, ~4300 AU in the morphants,). At 5 dpi, the fluorescence of bacterial burden reached ~9800 AU in the larvae treated with inhibitor, ~7200 AU in the control group and ~ 13560 AU upon morpholino knockdown(Fig.3A).

Transcriptomic profiling and gene ontology analysis in *M. marinum* infected larvae

To study the effects of *ptpn6* morpholino and NSC-87877 treatment on the transcriptional response to infection, we used morpholino- and NSC-87877-treated embryos infected with *M. marinum* and monitored them up to 5 dpf, when they were collected and used for further analysis. First, the larvae were used to study the *ptpn6* mRNA levels after *M. marinum* infection, which was measured using qRT-PCR analysis. The *ptpn6* expression was shown to be upregulated at 4 dpi, showing >7-fold increased *ptpn6* mRNA levels in the infected larvae compared to non-infected larvae (Fig.5A). Second, we compared transcriptomic profiles to study the effect of *ptpn6* morpholino- and NSC-87877 treatment on the transcriptional response to infection. We found 234 upregulated and 214 downregulated genes in the control infected group (Fig.5B). Interestingly, these numbers were more than ten-fold higher upon *ptpn6* morpholino and infection treatment (2417 and 2447 respectively) and NSC-87877 and infection treatment (3336 and 2496 respectively, Fig.5B). Volcano plots conformed this effect,

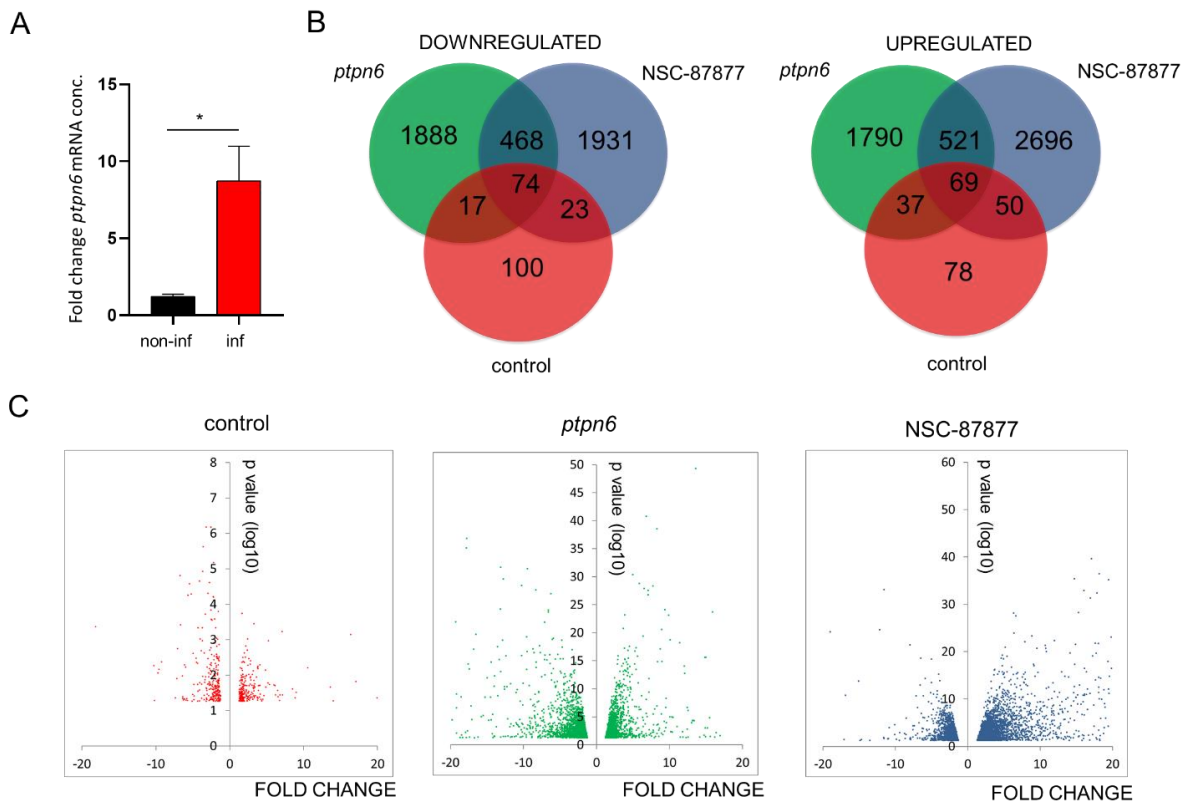

Figure 5. Transcriptome analysis by RNA-seq showing modulation of gene regulation induced by *ptpn6* MO knockdown and NSC-87877 treatment during *M. marinum* infection. **(A)** Expression of *ptpn6* at 5 dpi after *M. marinum* infection, determined using qRT-PCR. Data are mean ± s.e.m. from three independent experiments. Statistical significance is indicated by *P<0.05; (determined using student's t-test). **(B)** Venn diagrams showing significantly upregulated or downregulated genes during *M. marinum* infection in combination with control (red), *ptpn6* MO (green) and NSC-87877 (blue) treatment. **(C)** Volcano plots indicating the fold change (x-axis) and P-value (y-axis) of the regulation for individual genes.

showing dramatically larger variation in fold changes and p-values upon Ptpn6 inhibition (Fig.5C). The cluster of genes that was regulated by both morpholino/infection and NSC-87877/infection treatment, and not by the control/infection treatment included 989 genes (521 upregulated and 468 downregulated), which was only 11% of the total number of genes that are exclusively regulated upon Ptpn6 inhibition (Fig.5B).

We selected this cluster of shared 989 genes for further analysis. Gene ontology groups enriched in this cluster were mostly related to protein degradation for the upregulated genes, and synaptic transmission for the downregulated genes (Table 2). Analysis of enriched Kegg pathways revealed changes in MAPK,VEGF and p53 signaling pathways, which were found to be significantly upregulated in both *ptpn6* knockdown and NSC-87877 inhibited group, whereas some, such as purine metabolism were found to be downregulated (Table 3).

To further understand the effects of the *ptpn6* knockdown and NSC-87877 treatment on gene regulation, we manually analyzed the expression levels of the genes that are present in the signature sets of the *ptpn6* morpholino and NSC-87877 groups, but are not affected in the

control infection group. The analysis was performed using the Pathvisio software package (http://www.pathvisio.org). The most significant genes were grouped in immune response, matrix remodeling, prostaglandin, cytokine-cytokine receptor interaction and metabolic response (Fig.6).

Finally, analysis of several selected immune- and metabolism-related genes, described previously by Marín-Juez et al.[25], revealed that both Ptpn6 inhibition by NSC-87877 and *ptpn6* morpholino knockdown led to a stronger response from the immune system, with significant changes in the expression of *il1b, socs3a* and *socs3b*, and the largest increases in the expression of *irg1l, mmp9,* and *irak3* (Fig7A). The genes *tnfa* and *tnfb*, although highly induced after NSC-87877 inhibition, were not significantly changed by the *ptpn6* morpholino knockdown. Genes related to metabolism and protein degradation showed higher levels of regulation upon *ptpn6* morpholino treatment compared to NSC-87877 treatment. In the morpholino-treated group, an upregulation was observed for genes involved in insulin signaling pathway, such as *pck1*, *lepb* and *insb* as well as genes that play a role in protein degradation, such as *socs3a* and *fbxo32* (Fig.7B).

Discussion

Tyrosine (de)phosphorylation of proteins plays a critical role in the regulation of many immune-related processes. To study the role of the protein phosphatase PTPN6, we used zebrafish larvae as animal models and treated them with a small molecule inhibitor NSC-87877, that had previously been shown to inhibit human PTPN6 *in vitro*[26]. The effect of NSC-87877 treatment was compared with effects of morpholino knockdown of the *ptpn6* gene. Transcriptome analysis using RNA-seq of the non-infected *ptpn6* morpholino- and NSC-87877-treated groups identified enriched gene ontology groups of genes related to intermediate filaments and cell junctions, that are connected with skin structure and function. It has been previously been shown that *ptpn6* MO knockdown leads to inflammation, severe edema and skin lesions in zebrafish larvae[21], similar to the phenotypes that were found in murine Ptpn6 mutants *me*, *mev* and *spin*[39]. Moreover, Ptpn6^{spin} mice exhibit lesions that define neutrophilic dermatoses, including formation of intraepidermal pustules and cutaneous damage, associated with infiltrations with neutrophils[40]. However, the transcriptomes of non-infected *ptpn6* morphants and NSC-87877 treated larvae do not share many common genes that show regulation compared to the controls, and those that are shared are not obviously immune system- or neutrophil-related genes. Furthermore, within this cluster of these commonly regulated genes, enrichment of any specific pathway was not observed.

Table 2. Gene ontology analysis of the cluster of genes that are significantly regulated by ptpn6 MO/infection and NSC-87877/infection treatment and not by control/infection treatment using DAVID Functional Annotation Tool (Functional Annotation Clustering).

FUNCTIONAL ANNOTATION CLUSTERING		
Enrichment Score	UPREGULATED	DOWNREGULATED
7.24		Synapse Ion channel activity Cell junction GABA-A receptor complex Cell membrane
3.83	Protease Proteolysis Peptidase activity Hydrolase activity	
3.45	Protein catabolic process Proteasome ATPase TBP-class protein binding ER-associated ubiquitin Posttranslational modification	
3.29		Postsynaptic cell membrane NMDA receptor Glutamate receptor Extracellular ligand binding receptor
2.6	Endopeptidase activity Threonine protease	Nicotinic acetylcholine receptor Acetylcholine binding Cholinergic synaptic transmission
2.24	Hemoglobin complex Oxygen transport Globin Iron ion binding Heme	
2.19		Intermediate filament Structural molecule activity
2.06		Potassium transport Potassium channel BTB/POZ Voltage-gated channel

Table 3. Pathways analysis of the cluster of genes that are significantly regulated by ptpn6 MO/infection and NSC-87877/infection treatment and not by control/infection treatment using DAVID Functional Annotation Tool (Kegg pathways).

PATHWAYS	
UPREGULATED	DOWNREGULATED
Proteasome	Phototransduction
GnRH signaling pathway	Neuroactive ligand-receptor interaction
VEGF signaling pathway	Gap junction
p53 signaling pathway	Purine metabolism
Apoptosis	Calcium signaling pathway
Salmonella infection	
Regulation of actin cytoskeleton	
Glycine, serine and threonine metabolism	
MAPK signaling pathway	
Protein processing in endoplasmic reticulum	

Subsequently, we infected zebrafish embryos after both treatments with *M. marinum* mCherry fluorescent strain to explore the role of Ptpn6 in the response to a bacterial infection. Our results support previous results showing that reduced Ptpn6 activity impairs the ability of zebrafish embryos to control mycobacterial infection. Our data showed that the effect of NSC-87877 treatment on the bacterial burden was milder than the effect of *ptpn6* MO knockdown and resulted in lower mortality ratios. This difference in mortality might be connected with inhibition of the related protein phosphatase Ptpn11 by NSC-87877, as in murine cells PTPN11 has been shown to play a negative role in cell survival during inflammation and to accelerate apoptosis through the dephosphorylation of signal transducer and activator of transcription 5 (STAT5)[41]. At the transcriptional level, we found that the combination of either *ptpn6* MO or NSC-87877 treatment and infection regulated approximately ten-fold more genes than the infection in control larvae. Amon the genes that were regulated by both combination treatments and not in the control larvae we observed

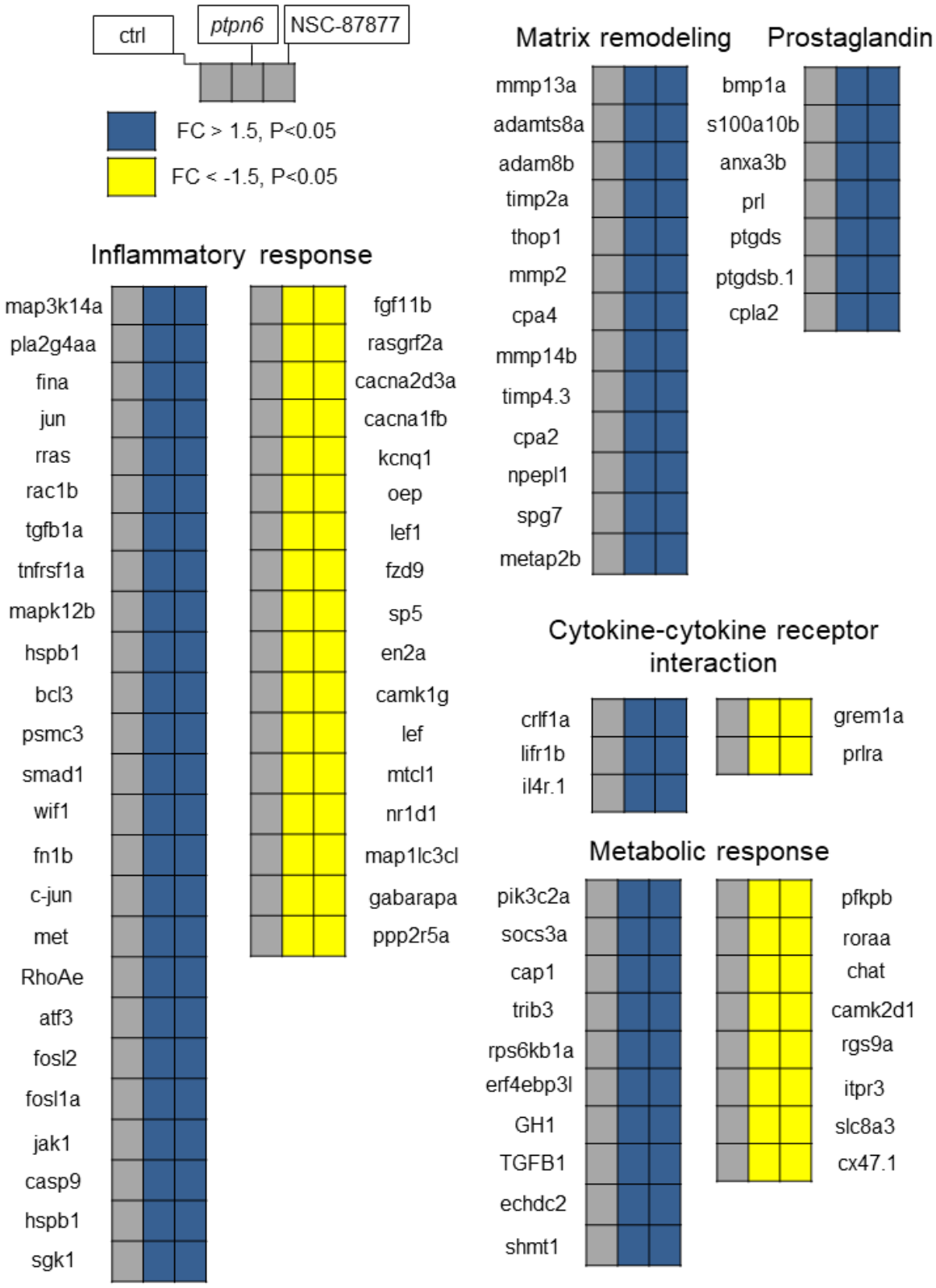

Figure 6. RNA-seq results for selected immune- and metabolism-related genes showing modulation of gene regulation by *ptpn6* MO knockdown and NSC-87877 treatment during *M. marinum* infection. Regulation is shown for the control infection experiment (left box), *ptpn6* MO infection experiment (middle box), and the NSC-87877 infection experiment (right box). Ratios are given for the infected versus the non-infection control group for each experiment. Blue boxes represent upregulation, yellow boxes represent downregulation, yellow boxes represent downregulation of gene expression.

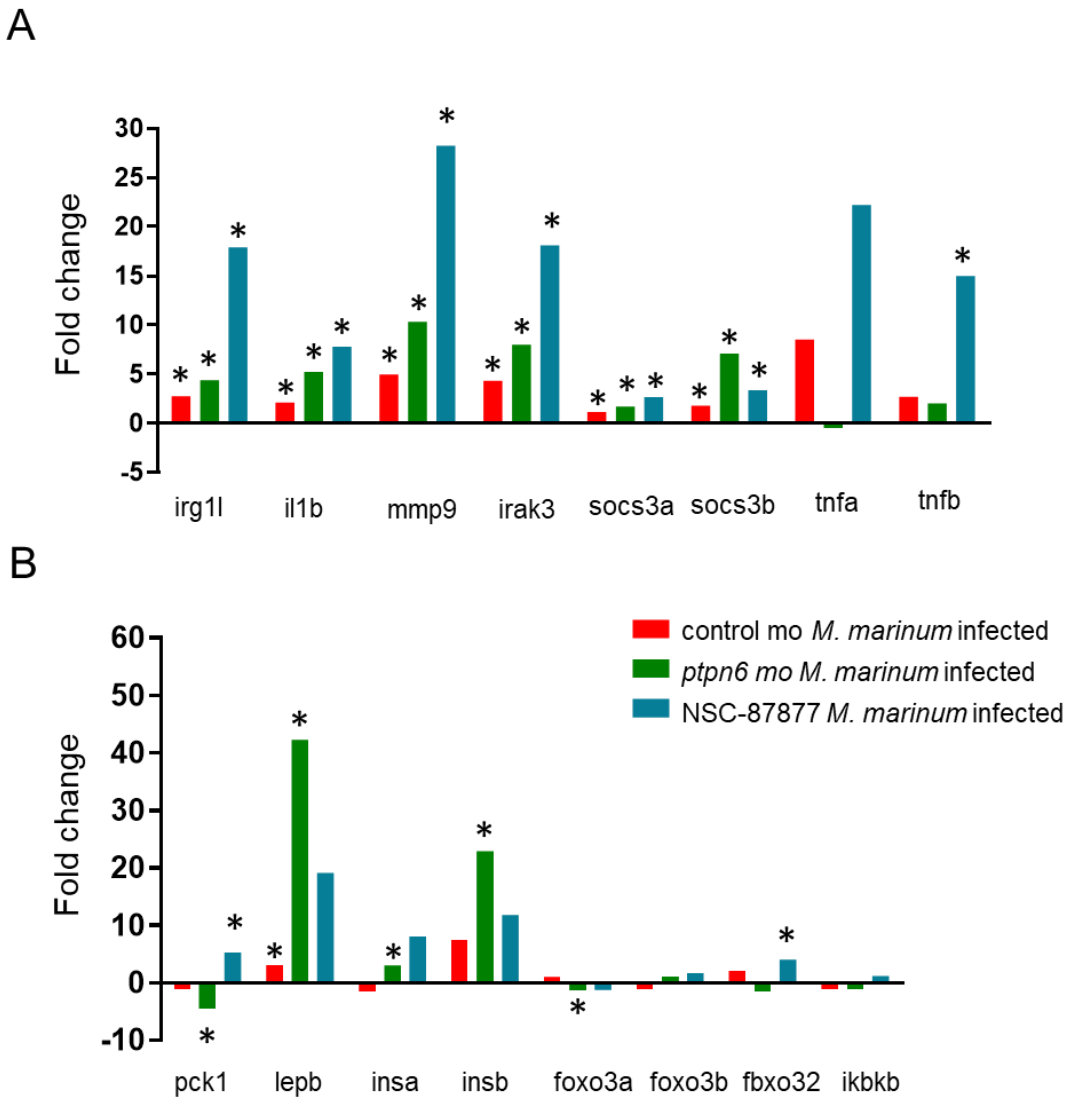

Figure 7. RNA-seq results for selected immune- and metabolism-related genes showing levels of gene regulation. The level of regulation (fold change) is shown in the control/infection (red bars), *ptpn6* MO/infection (green bars), and NSC-87877/infection (blue bars) groups compared to the control/non-infection group. Regulation of a selection of genes previously identified to be involved in innate immunity **(A)** and metabolism **(B)** is presented. Statistical significance (determined using analysis by Genetiles software) is indicated by *P<0.05

an enrichment of genes involved in synaptic transmission, ion transport, cell structure and proteolysis. Significantly changed pathways showed similar pattern with upregulation in some immune and inflammatory related pathways, cell structure and hormone release. Pathways related to synaptic transmission and transport were found to be downregulated. Dysregulation of MAPK signaling pathway and enhanced apoptosis were described previously in *ptpn6* morphants by Kanwal et al.[21], which corresponds with our findings.

Analysis of the regulation of various selected immune-related genes showed that both *ptpn6* MO knockdown and NSC-87877 treatment enhanced the expression of various genes involved in the innate immune response after *M. marinum* infection. We found that the most significantly upregulated immune-related gene after mycobacterial infection and NSC-87877

or *ptpn6* morpholino treatment was *mmp9*. Previous studies in zebrafish showed that *mmp9* is a crucial pro-inflammatory marker, which becomes highly induced by bacterial infection[42,43]. Other genes involved in immune processes that were also more highly induced after both *ptpn6* morpholino and NSC-87877 treatment were *irak3, irg1l, il1b, socs3a* and *socs3b*. These findings correspond with the data obtained by Kanwal et al.[21], who showed that *ptpn6* MO knockdown in zebrafish larvae infected with *S. typhimurium* resulted in hyperinduction of *mmp9* and *il1b*. These results suggest that *ptpn6* acts as a negative regulator of pro-inflammatory genes during the response to a bacterial infection. However, the results show some differences that are probably due to the fact that the microarray analysis performed by Kanwal et al.[21] were based on *Salmonella typhimurium* infection studies. Comparison of the results suggests that Ptpn6 has a stronger role in controlling responses to *S. typhimurium* infection than to *M. marinum* infection.

The most upregulated gene by the *ptpn6* MO/infection treatment that was also upregulated in the NSC-878777/infection group was *leptin b* that has previously been shown to be linked to *ptpn6* function (this thesis, Chapter 3) and to play both an immunological and metabolic role. This finding was not a surprise since previous studies in zebrafish larvae have already shown that *leptin b* becomes highly induced by mycobacterial infection[35]. Marín-Juez et al.[25] have suggested that Ptpn6 inhibits the leptin signaling pathway thereby suppressing the immune response. This conclusion was based on the studies where stimulation of PTPN6 by insulin led to JAK2 dephosphorylation, therefore interfering with the leptin signaling pathway[25]. Our finding that decreased Ptpn6 function caused hyperexpression of *leptin b* supports this hypothesis.

Most of the similarities between the *ptpn6* MO and the NSC-87877 treatments during infection were found in the group of genes involved in synaptic transmission, ion transport, cell structure, proteolysis, immune response, apoptosis and hormone release. However, there were differences in the regulation of the expression levels of many metabolic genes. In general, *ptpn6* MO/infection treatment had more impact on metabolic genes than NSC-87877/infection treatment. For instance, genes significantly changed by *ptpn6* MO knockdown were *insa*, *insb, pck1, fbxo32* and *foxo3a,* and these genes were not significantly regulated by NSC-87877. These genes are known to play a crucial role in the insulin signaling pathway and may play a role in the development of diabetes mellitus[44]. The mechanism behind the differences in the gene expression levels between the *ptpn6* MO- and NSC-87877-treated groups still remains unclear. NSC-87877 administration leads to stronger upregulation of expression of genes encoding cytokines and other immune-related proteins, its enhancement of the bacterial infection in zebrafish larvae is less severe than *ptpn6* MO knockdown. Administration of the *ptpn6* MO may resulted in several off-target effects and toxicity, which can result in an increased bacterial burden and mortality of the infected larvae. Relatively higher expression levels of immune-related genes and lower expression of some metabolic genes after treatment with NSC-87877 might be the result of a combination of both Ptpn6 and Ptpn11 inhibition. Knockout of *Ptpn11* in mice led to overproduction of the pro-

inflammatory cytokines IL-1β and IL-18 and increased sensitivity to peritonitis. In the mice with peritonitis, the infection showed a more severe course and was associated with excessive inflammasome activation[45]. Both PTPN6 and PTPN11 have been shown to modulate the insulin signaling pathway[25,46,47], which is in line with our observation of differences in the expression of metabolic genes, mainly involved in the insulin signaling pathway. Indeed, knockdown of *ptpn6* in zebrafish larvae has been shown to improve glucose uptake upon administration of a high dose insulin[25], whereas it was also shown that inhibition of PTPN11 in diabetic rats resulted in improved glucose uptake and reversed other diabetic alterations[46].

In summary, in the present study, we have compared *ptpn6* knockdown using morpholino oligonucleotides and Ptpn6 inhibition using NSC-87877, a non-specific PTPN6 inhibitor. Infection data show that both methods of decreasing Ptpn6 function compromises the defense against mycobacterial infection. Although we found some differences between the two treatments, we showed that the effects of these treatments show interesting similarities. The set of genes that show the same transcriptional response upon either treatment is a useful reference set that can specifically linked to the function of Ptpn6.

Supplementary materials

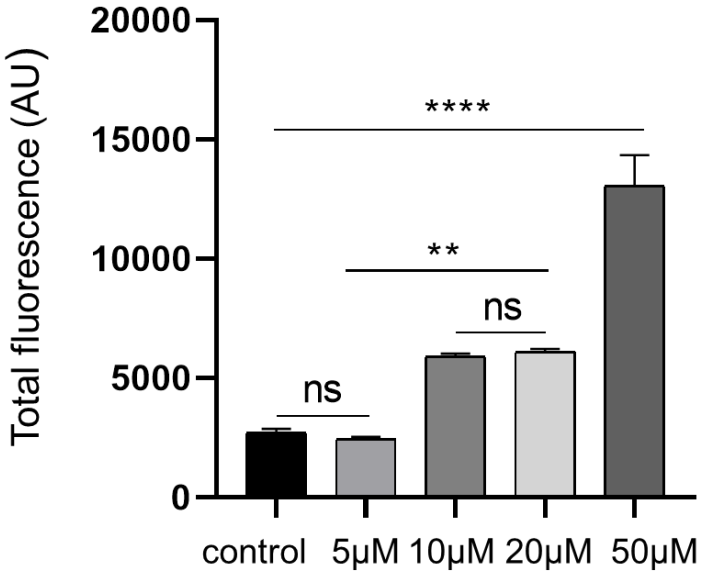

Supplementary Figure 1. Pixel counting of bacterial burden in the control/infection and NSC-87877/infection groups at 5 dpi. NSC-87877 was used in the concentrations of 5 μM, 10 μM, 20 μM and 50 μM. Data shown are means ± s.e.m. from three independent experiments. Statistical significance is indicated by: **P<0.01; ***P<0.0001; (determined using ANOVA with Tukey's post hoc test).

References

1. He RJ, Yu ZH, Zhang RY, Zhang ZY. 2014; Protein Tyrosine Phosphatases as Potential Therapeutic Targets. Acta Pharmacol Sin. 35(10):1227-46.
2. Hoppstädter J, Ammit AJ. 2019; Role of Dual-Specificity Phosphatase 1 in Glucocorticoid-Driven Anti-inflammatory Responses. Front Immunol. 10:1446.
3. Jiménez-Martínez M, Stamatakis K, Fresno M. 2019; The Dual-Specificity Phosphatase 10 (DUSP10): Its Role in Cancer, Inflammation, and Immunity. Int J Mol Sci. 20(7).
4. Julien SG, Dubé N, Hardy S, Tremblay ML. 2011; Inside the human cancer tyrosine phosphatome. Nat Rev Cancer. 11(1):35-49.
5. Tonks NK. 2013; Protein tyrosine phosphatases-from housekeeping enzymes to master regulators of signal transduction. FEBS J. 280(2):346-78.
6. Garg M, Wahid M, Khan F. 2019; Regulation of peripheral and central immunity: Understanding the role of Src homology 2 domain-containing tyrosine phosphatases, SHP-1 & SHP-2. Immunobiology. 6:151847.
7. Liu Q, Qu J, Zhao M, Xu Q, Sun Y. 2019; Targeting SHP2 as a promising strategy for cancer immunotherapy. Pharmacol Res. 152:104595.
8. Niogret C, Birchmeier W, Guarda G. 2019; SHP-2 in Lymphocytes' Cytokine and Inhibitory Receptor Signaling. Front Immunol. 10:2468.
9. Tonks NK. 2006; Protein tyrosine phosphatases: from genes, to function, to disease. Nat Rev Mol Cell Biol. 7(11):833-46.
10. Zhang J, Somani AK, Siminovitch KA. 2000; Roles of the SHP-1 tyrosine phosphatase in the negative regulation of cell signalling. Semin. Immunol. 12: 361–378.
11. Plutzky J, Neel BG, Rosenberg RD. 1992; Isolation of a src homology 2-containing tyrosine phosphatase. Proc Natl Acad Sci USA. 89(3):1123-7.
12. Tsui HW, Hasselblatt K, Martin A, Mok SC, Tsui FW. 2002; Molecular mechanisms underlying SHP-1 gene expression. Eur J Biochem. 269(12):3057-64.
13. Grossmann KS, Rosário M, Birchmeier C, Birchmeier W. 2010; The tyrosine phosphatase Shp2 in development and cancer. Adv Cancer Res. 106():53-89.
14. Immunological Genome Project, https://www.immgen.org
15. Abram CL, Lowell CA. 2017; Shp1 function in myeloid cells. J Leukoc Biol. 102(3):657-675.
16. Shultz LD, Rajan TV, Greiner DL. 1997; Severe defects in immunity and hematopoiesis caused by SHP-1 protein-tyrosine-phosphatase deficiency. Trends Biotechnol. 15:302–307.
17. Green MC, Shultz LD. 1975; Motheaten, an immunodeficient mutant of the mouse. I. Genetics and pathology. J Hered. 66(5):250-8.
18. Sharma Y, Bashir S, Bhardwaj P, Ahmad A, Khan F. 2016; Protein tyrosine phosphatase SHP-1: resurgence as new drug target for human autoimmune disorders. Immunol Res. 64(4):804-19.

19. Yu CC, Tsui HW, Ngan BY, Shulman MJ, Wu GE, Tsui FW. 1996; B and T cells are not required for the viable motheaten phenotype. J Exp Med. 183(2):371-80.
20. Lam SH, Chua HL, Gong Z, Lam TL, Sin YM. 2004; Development and maturation of the immune system in zebrafish, Danio rerio: a gene expression profiling, in situ hybridization and immunological study. Dev. Comp. Immunol. 28: 9–28.
21. Kanwal Z, Zakrzewska A, den Hertog J, Spaink HP, Schaaf MJ, Meijer AH. 2013; Deficiency in hematopoietic phosphatase ptpn6/Shp1 hyperactivates the innate immune system and impairs control of bacterial infections in zebrafish embryos. J Immunol. 190(4):1631-45.
22. Westerfield, M. 2000; The Zebrafish Book. A Guide for the Laboratory Use of Zebrafish (*Danio rerio*). (Eugene: University of Oregon Press).
23. Davis JM, Clay H, Lewis JL, Ghori N, Herbomel P, Ramakrishnan L. 2002; Real-time visualization of mycobacterium-macrophage interactions leading to initiation of granuloma formation in zebrafish embryos. Immunity. 17(6):693-702.
24. Willett CE, Cortes A, Zuasti A, Zapata AG. 1999; Early hematopoiesis and developing lymphoid organs in the zebrafish. Dev Dyn. 214(4):323-36.
25. Marín-Juez R, Jong-Raadsen S, Yang S, Spaink HP. 2014; Hyperinsulinemia induces insulin resistance and immune suppression via Ptpn6/Shp1 in zebrafish. J Endocrinol. 222(2):229-41.
26. Chen L, Sung S, Yip M, Lawrence H. 2006; Discovery of a novel SHP-2 protein tyrosine phosphatase inhibitor. Mol. Pharmacol. 70: 562–570.
27. Pinzon-Guzman C, Xing T, Zhang SSM, Barnstable CJ. 2015; Regulation of Rod Photoreceptor Differentiation by STAT3 Is Controlled by a Tyrosine Phosphatase. J Mol Neurosci. 55(1):152-159.
28. Raghav PK, Singh AK, Gangenahalli G. 2018; Stem cell factor and NSC-87877 combine to enhance c-Kit mediated proliferation of human megakaryoblastic cells. PLoS One. 13(11):e0206364.
29. Shi Y, Ma IT, Patel RH, Shang X, Chen Z, Zhao Y, Cheng J, Fan Y, Rojas Y, Barbieri E, Chen Z, Yu Y, Jin J, Kim ES, Shohet JM, Vasudevan SA, Yang J. 2015; NSC-87877 inhibits DUSP26 function in neuroblastoma resulting in p53-mediated apoptosis. Cell Death Dis.6:e1841.
30. Song M, Park JE, Park SG, Lee DH, Choi HK, Park BC, Ryu SE, Kim JH, Cho S. 2009; NSC-87877, inhibitor of SHP-1/2 PTPs, inhibits dual-specificity phosphatase 26 (DUSP26). Biochem Biophys Res Commun. 381(4):491-5.
31. Spaink HP, Cui C, Wiweger MI, Jansen HJ, Veneman WJ, Marín-Juez R, de Sonneville J, Ordas A, Torraca V, van der Ent W, Leenders WP, Meijer AH, Snaar-Jagalska BE, Dirks RP. 2013; Robotic injection of zebrafish embryos for high-throughput screening in disease models. Methods. 62(3):246-54.
32. Carvalho R, de Sonneville J, Stockhammer OW, Savage ND, Veneman WJ, Ottenhoff TH, Dirks RP, Meijer AH, Spaink HP. 2011; A High-Throughput Screen for Tuberculosis Progression. PLoS One. 6(2): e16779.

33. Benard EL, van der Sar AM, Ellett F, Lieschke GJ, Spaink HP, Meijer AH. 2012; Infection of zebrafish embryos with intracellular bacterial pathogens. J Vis Exp.(61).
34. Stoop EJ, Schipper T, Rosendahl Huber SK, Nezhinsky AE, Verbeek FJ, Gurcha SS, Besra GS, Vandenbroucke-Grauls CM, Bitter W, van der Sar AM. 2011; Zebrafish embryo screen for mycobacterial genes involved in the initiation of granuloma formation reveals a newly identified ESX-1 component. Dis Model Mech. 4(4):526-36.
35. Veneman WJ, de Sonneville J, van der Kolk KJ, Ordas A, Al-Ars Z, Meijer AH, Spaink HP. 2015; Analysis of RNAseq datasets from a comparative infectious disease zebrafish model using GeneTiles bioinformatics. Immunogenetics. 67(3):135-47.
36. Pico AR, Kelder T, Iersel MP, Hanspers K, Conklin BR, Evelo C. 2008; WikiPathways: pathway editing for the people. PLoS Biol. 6(7):e184.
37. Hochberg Y, Benjamini Y. 1990; More Powerful Procedures for Multiple Significance Testing. Stat Med. 9(7):811-8.
38. Huang da W, Sherman BT, Lempicki RA. 2009; Systematic and integrative analysis of large gene lists using DAVID bioinformatics resources. Nat Protoc. 4:44–57.
39. Shultz LD, Schweitzer PA, Rajan TV, Yi T, Ihle JN, Matthews RJ, Thomas ML, Beier DR. 1993; Mutations at the murine motheaten locus are within the hematopoietic cell protein-tyrosine phosphatase (Hcph) gene. Cell 73: 1445–1454.
40. Nesterovitch AB, Gyorfy Z, Hoffman MD, Moore EC, Elbuluk N, Tryniszewska B, Rauch TA, Simon M, Kang S, Fisher GJ, Mikecz K, Tharp MD, Glant TT. 2011; Alteration in the gene encoding protein tyrosine phosphatase nonreceptor type 6 (PTPN6/SHP1) may contribute to neutrophilic dermatoses. Am J Pathol. 178(4):1434-41.
41. Chen J, Yu WM, Bunting KD, Qu CK. 2004; A negative role of SHP-2 tyrosine phosphatase in growth factor-dependent hematopoietic cell survival. Oncogene. 23(20):3659-69.
42. van der Vaart M, Korbee CJ, Lamers GE, Tengeler AC, Hosseini R, Haks MC, Ottenhoff TH, Spaink HP, Meijer AH. 2014; The DNA damage-regulated autophagy modulator DRAM1 links mycobacterial recognition via TLR-MYD88 to autophagic defense. Cell Host Microbe. 15(6):753-67.
43. Volkman HE, Pozos TC, Zheng J, Davis JM, Rawls JF, Ramakrishnan L. 2010; Tuberculous granuloma induction via interaction of a bacterial secreted protein with host epithelium. Science. 327(5964):466-9.
44. O'Neill BT, Bhardwaj G, Penniman CM, Krumpoch MT, Suarez Beltran PA, Klaus K, Poro K, Li M, Pan H, Dreyfuss JM, Nair KS, Kahn CR. 2019; FoxO Transcription Factors Are Critical Regulators of Diabetes-Related Muscle Atrophy. Diabetes. 68(3): 556–570.
45. Guo W, Liu W, Chen Z, Gu Y, Peng S, Shen L, Shen Y, Wang X, Feng GS, Sun Y, Xu Q. 2017; Tyrosine phosphatase SHP2 negatively regulates NLRP3 inflammasome activation via ANT1- dependent mitochondrial homeostasis. Nat Commun. 8(1):2168.

46. Yue X, Han T, Hao W, Wang M, Fu Y. 2020; SHP2 knockdown ameliorates liver insulin resistance by activating IRS-2 phosphorylation through the AKT and ERK1/2 signaling pathways. FEBS Open Bio.
47. Andersen JN, Jansen PG, Echwald SM, Mortensen OH, Fukada T, Del Vecchio R, Tonks NK, Møller NP. 2004; A genomic perspective on protein tyrosine phosphatases: gene structure, pseudogenes, and genetic disease linkage. FASEB J. 18(1):8-30.